

Experimental and Numerical Modeling of Tsunami Force on Bridge Decks

Tze Liang Lau¹, Tatsuo Ohmachi²,
Shusaku Inoue² and Panitan Lukkunaprasit³

¹*Universiti Sains Malaysia*

²*Tokyo Institute of Technology*

³*Chulalongkorn University*

¹*Malaysia*

²*Japan*

³*Thailand*

1. Introduction

Tsunamis are destructive waves which contain a series of long period waves. These waves propagate at very high speed and travel transoceanic distance with very little energy losses. When tsunamis approach a shore, their tremendous energy remains nearly unchanged and the high inundation level and the fast moving water of tsunami flow cause loss of human lives and catastrophe to coastal structures including bridges (Figure 1). The extensive bridge damage caused by recent tsunamis in particularly in the unprecedented 2004 Indian Ocean tsunami event demonstrates an urgent need for an effective method to estimate tsunami forces on bridges.

Due to the complexity of wave propagation on shore and wave-structure interaction, physical and numerical approaches have been adopted to investigate tsunami-induced forces on bridges. Even though tsunami force acting on vertical wall-type coastal structures has been studied by many researchers since last five decades, but the assessment of tsunami force on bridge is still in its early stage. There has still no conclusive argument on how big tsunamis are. The occurrence of the 2004 Indian Ocean tsunami shows the enormous force exerted by the tsunami which had floated a 10-MW barge-mounted diesel station 3 km inland in Banda Aceh, shifted a heavy dredger onto the wharves in Sri Lanka and drifted a police patrol boat 1.2 km inland in Thailand. This disastrous wave force is once again shown in the most recent tsunami triggered by the 2011 Tohoku Region Pacific Ocean Offshore Earthquake.

The post-tsunami survey have evidently demonstrated the damage of bridges in Sumatra, Sri Lanka, India and Thailand during the 2004 tsunami event as reported by Kusakabe et al. (2005), Unjoh (2005), Iemura et al. (2005), Yim (2005), Saatcioglu et al., (2005), Tobita et al., (2006), Ballantyne (2006), Maheshwari et al. (2006), Scawthorn et al. (2006), Sheth et al. (2006), EEFIT (2006) and IIT (2011). These bridges suffered failure through a total or partial wash-away of bridge deck from their abutments and excessive settlement of foundation. The failure of bridges disrupts the accessibility of the community; nevertheless, the great concern is hamper the emergency relief efforts that are needed immediately after this disastrous event.



(a) Total Wash-Away of Deck (Unjoh, 2005) (b) Excessive Deck Displacement (Yim, 2005)

Fig. 1. Bridge damage due to tsunami attack in Banda Aceh

The report on the post-tsunami survey done by a team from Japan Society of Civil Engineers (Unjoh, 2005) has stated that more than 100 bridges in which their superstructures were washed out or heavily damaged by tsunami with a height of 5 m to over 30 m in Aceh Province. Out of these bridges, there are simple supported reinforced concrete bridges, prestressed concrete bridges and steel truss bridges. Indian Institute of Technology Kanpur reconnaissance team discovered several bridges in Andaman and Nicobar Islands were heavily damaged (IIT, 2011). Three road bridges and two railway bridges suffered severe damage and some bridges suffered damages to abutments and approaches in Sri Lanka while no apparent damage to reinforced concrete bridges in Thailand was reported by EEFIT (2006). About four bridges suffered severe damage in India (Sheth et al., 2006). A four span reinforced concrete bridge across Palyar River in India was totally washed away (Narayan et al., 2005; Jain et al., 2005).

2. Damage mechanism of bridges

Various types of damage on bridges have been demonstrated in past events through post-tsunami survey. It can be categorized into two main types, i.e. damage to substructure and superstructure. Damage to bridge substructure can be resulted from scouring of foundation and excessive settlement of the embankment whereas damage to bridge superstructure range from partial transverse movement of bridge deck to total collapse or wash out of bridge deck due to the action of both horizontal and uplift forces. The extent of bridge damage is closely related to the shape or form of the structure apart from the wave height and wave velocity which are topographic dependent.

2.1 Damage to bridge substructure

Tsunami with high flow velocity can erode the embankment of bridges if no sufficient protection is provided. This can cause the access road approaches the bridge disconnected or the settlement of bridge abutment. Collapse due to erosion and scour damage to the abutment should be prevented on the seaward side from the incoming wave attack and on the landward side from the receding water.

2.2 Damage to bridge superstructure

Most of the bridges constructed in countries surround the Indian Ocean are not designed to withstand large lateral load such as tsunami. Bridges are simply supported on abutments without any installation of shear key or other lateral movement restrainers. When tsunami strikes the bridge deck, the huge force can displace the deck laterally once the resistance due to friction is exceeded. The deck may experience substantial dislocation and the whole deck will be washed away from the abutment. Uplift force and hydrodynamic force contribute to this failure mechanism. If the bridge deck is submerged into the water during tsunami attack, the deck can be floated due to buoyant force and only minimum hydrodynamic force is sufficient to move the bridge deck.

3. Hydraulic experiments

Numerous researches have been carried out to investigate the behavior of bridges and estimate tsunami forces on bridges through physical modeling in recent years. As a result of the paucity of the tsunami wave force study on bridges and the complexity of tsunami propagation at nearshore region, physical modeling was carried out to investigate the occurrence of tsunami acting on an inland bridge. Hydraulic experiments in various scales of wave flume were conducted using various configurations of downscaled bridge models.

3.1 Reviews on related experimental studies

Experimental studies of tsunami forces on bridges have only been conducted after the unprecedented 2004 Indian Ocean tsunami event by Kataoka et al. (2006), Shoji & Mori (2006), Iemura et al. (2007), Lau et al. (2008), Sugimoto et al. (2008), Moriyama et al. (2008), Araki et al. (2008 and 2010), Shoji et al., (2009a, 2009b and 2010), Nakao et al. (2009) and Nii et al. (2009 and 2010). All these studies employed rigid bed models. Various model scales from 1/18 to 1/150 were adopted.

Previous researchers omitted the piers or making piers sizes un-proportionally small in the physical models as done by previous researchers, they essentially ignore the influence of the piers and deck on the flow condition around each individual component. Therefore, a more realistic model was employed in this research which included both the piers and decks in the actual proportion. The experimental results show that the presence of bridge deck in a complete pier-deck model can increase the hydrodynamic pressure acting on the pier as much as 50 % than the one calculated based on the stand-alone pier model (Lukkunaprasit & Lau, 2011).

3.2 Experimental study

The basic principle of physical modeling is to simulate the characteristics of the prototype by the model which is generally at a reduced scale under certain similitude criterion. A wave flume experiment was conducted to obtain the time histories of pressures and forces on an inland bridge model subjected to tsunami loading.

3.2.1 Experimental setup

Figure 2 illustrates the setup of this experimental study. The hydraulic model experiments were carried out in a wave flume of 1 m × 1m in cross section and 40 m in length. The rigid bed of the flume with a compound bed slope of 1/115 (0.5°) and a flat platform where the model is located was constructed from painted steel plates supported by structural steel

sections. The coastal geometry was downscaled in the model study with the length scale of 1/100.

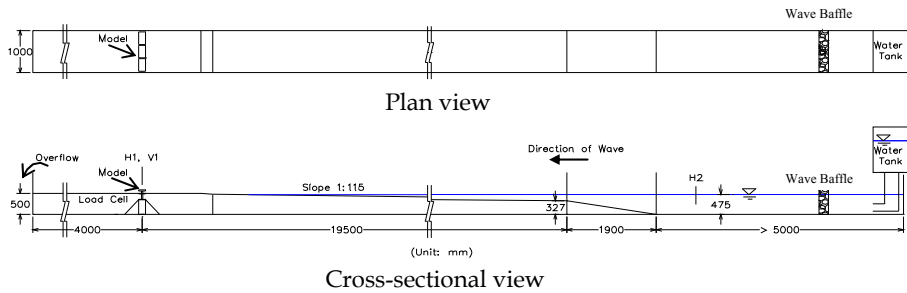


Fig. 2. Schematic diagram of the experimental setup

The water stored in the elevated tank at the farthest right end of the flume in Figure 2 was released abruptly in order to generate a tsunami-like solitary wave. Solitary-like waves with different wave heights were generated by varying the amount of released volume of water. Figure 3a shows a single solitary wave that was formed at the location near to offshore region (H2). The wave with almost a vertical wave front (Figure 3b) broke in the finite depth of still-water as a plunging-type breaker (Figure 3c) after losing its stability. The wave then transformed into bore by shoaling a solitary wave at a distance of about 20 m offshore. The turbulent bore runup on shore takes the form of a surge (as described by Camfield (1994) and Yeh (2007)) striking the bridge model which is rigidly installed at the downstream end of the flume.

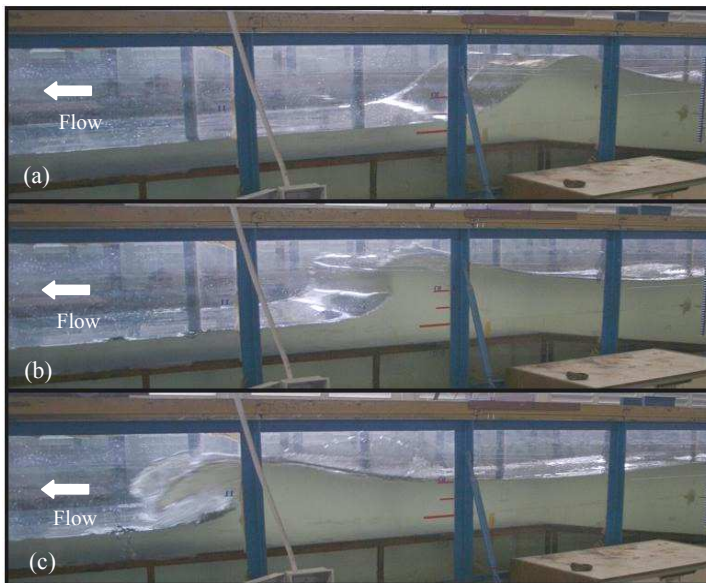


Fig. 3. Simulated tsunami wave

3.2.2 Target bridge and bridge model

The target bridge prototype is a reinforced concrete bridge with I-beam girder which is widely constructed in countries surround the Indian Ocean. The bridge, spanning 30 m apart, consists of a deck 13.8 m wide supported by 1.5 m deep girders, and 1 m high parapets. The deck clearance (height from the ground to the girder soffit) is 5.6 m. A ground level of 2.5 m above the mean sea level is considered. The expected tsunami inundation depth at the site is about 8 m with reference to the ground and the wave hits perpendicularly to the longitudinal axis of the bridge. Since the tsunami force is normally not taken into consideration during the design of inland bridges, these structures are highly vulnerable to damage should a tsunami attack.

The 1/100 scaled complete pier-deck bridge model constructed from clear acrylic plates was mounted on a base plate flushes with the surrounding dry bed located downstream. Figure 4 illustrates the typical cross-sectional and front views of the bridge models, respectively. Three spans of the bridge deck with each span of 138 mm in width by 300 mm in length were installed across the width of the flume and perpendicular to the flow direction. Out of these three spans, only the middle span was instrumented with pressure gauges and a load cell. The model included the bridge piers spaced at 137 mm apart. The base plate was mounted on a high frequency load cell which was used to record the total horizontal wave forces acting on the complete pier-deck bridge model. Also shown in the figures are the positions of pressure gauges on the model. P₁ designates the pressure gauge location at the base of the pier while P₂, P₃ and P₄ are those at the mid-span of girders G1, G2 and G3, respectively.

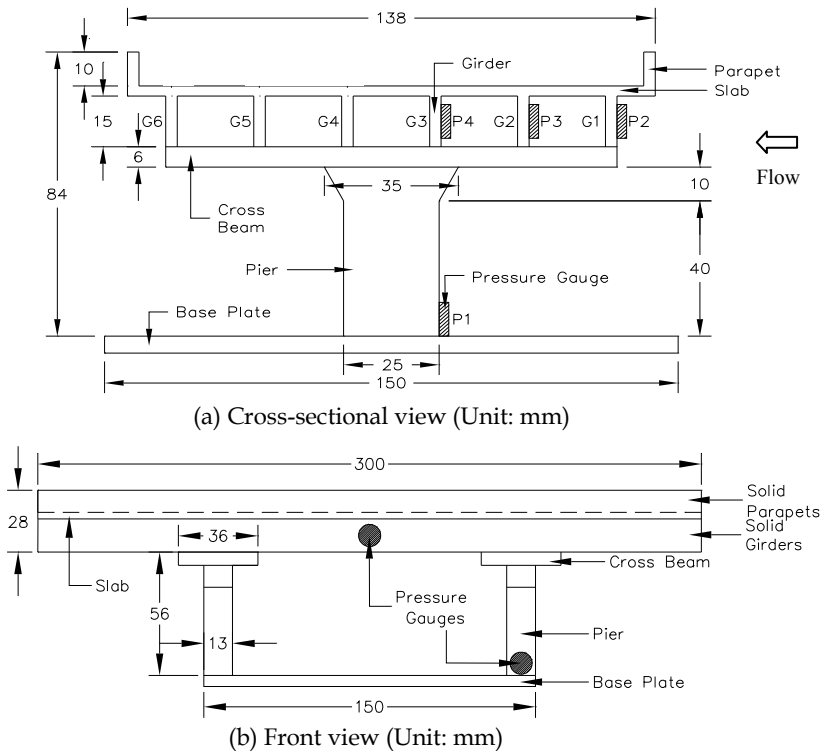


Fig. 4. Bridge model

3.2.3 Instrumentation

Capacitance type wave gauges were used to measure the wave profiles at onshore (H1) and offshore (H2) locations as illustrated in Figure 2. The velocities of the flow in the flume for various wave heights were recorded by a propeller type current meter at V1 (Figure 2). Both wave gauge and current meter were installed at H1 and V1 with the absence of the model during measurement. During the testing of the model, only the wave height at H2 was measured in order to avoid the interference from the instruments on the flow regime in the vicinity of the model. Tsunami forces in the horizontal direction were measured by a calibrated high frequency load cell which was mounted at the base of the bridge model. The recorded value from the load cell represented the total horizontal wave forces acting on the deck and the piers as a result of the wave pressure and the drag. The wave pressures were measured by miniature pressure gauges with high frequency response.

3.3 Measured time histories of forces and pressures

The typical time histories of the velocity and the height of the wave at the location of the bridge model (in the absence of the model) are depicted in Figure 5. The instant when the wave first hits the bridge model is taken as $t = 0$. It is to be noted that the leading edge of the wave attains a practically maximum velocity at the instant it reaches the location of the bridge model when the wave height is still very small. As the wave increases in height, the velocity decreases significantly, and the maximum wave height is attained at some time later than the instant the velocity is maximum. Therefore, the peak flow velocity does not coincide with the maximum wave height.

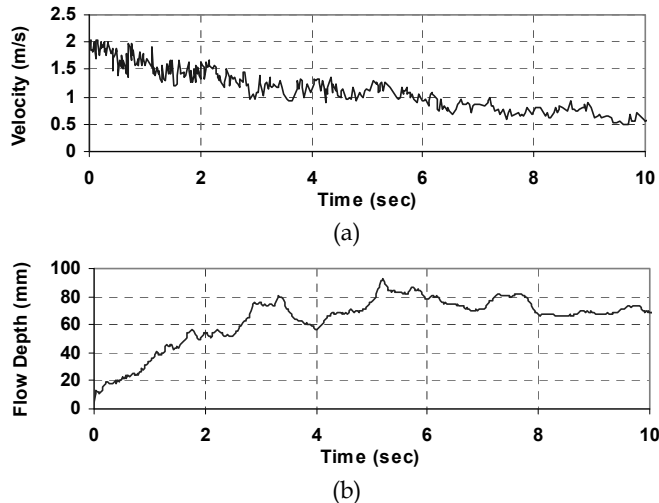


Fig. 5. Measured time histories of flow depth and velocity

Figures 6 and 7 present typical time histories of the wave force and wave pressures measured. As the leading edge of the wave (Figure 8a) strikes the bottom of the bridge piers with a high velocity, part of the upward splash hits the soffit of the cross beams while the remaining splash is diverted sideways. The pressure gauge reading P1 (at the pier) almost instantaneously attains the peak value (more than 3 times the hydrostatic pressure as shown in Figure 7a) while no pressure is recorded at the girders. At this instant, the wave height

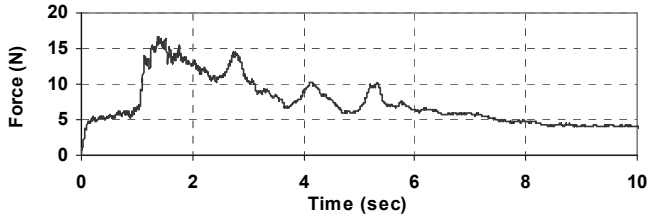


Fig. 6. Measured time histories of force

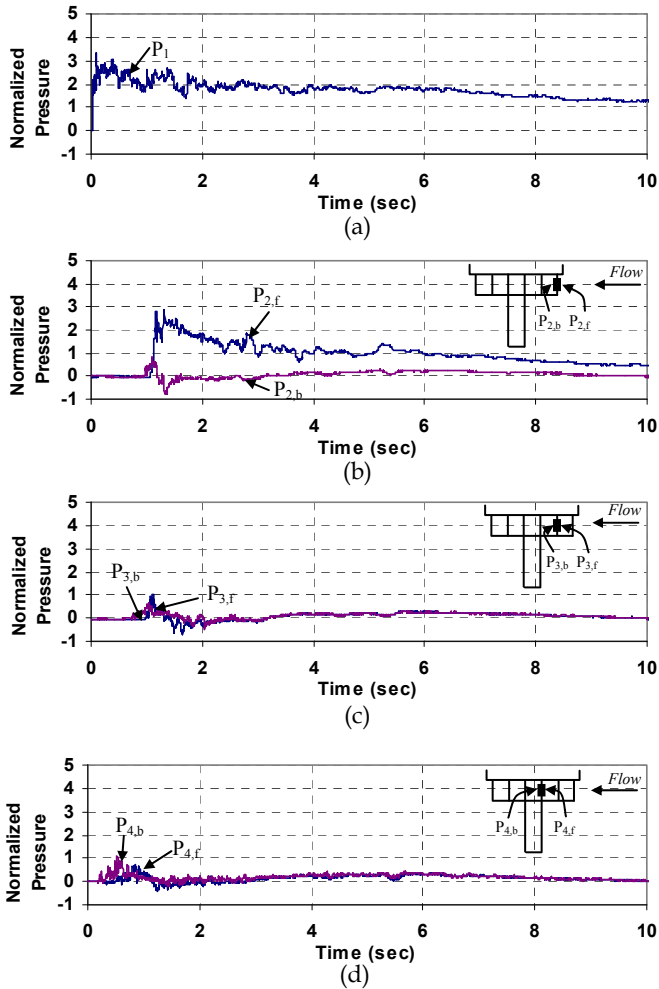


Fig. 7. Measured time histories of pressures

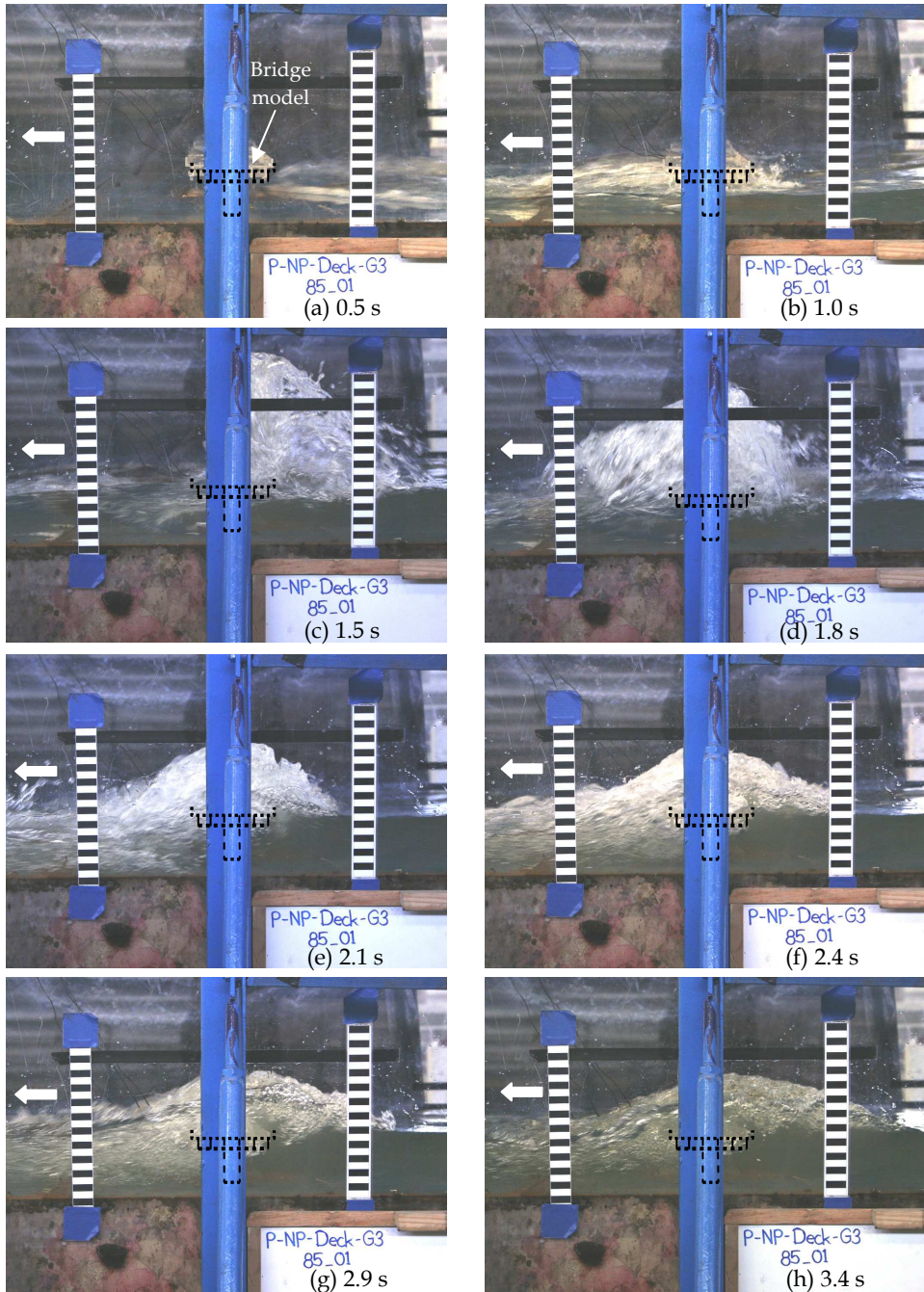


Fig. 8. Sequential events of wave impingement on a model bridge from experiment

and the wave force are relatively small, but they increase rapidly with time, and the force records the first peak value of 5.5 N at second 0.3 (Figure 6). These forces may be regarded as the peak forces on the piers. Thereafter the wave height increases but the velocity decreases as mentioned earlier with the result of the force being sustained near the peak value for nearly one second.

The pressures on the girders remain zero (except P4 which is most likely due to the minor splash-up) until the height of the wave rises to the lower part of the bridge girders (Figure 8b) when the wave splashes over the bridge deck with a height of three times that of the incident wave as shown in Figure 8c. This results in a rapid increase of wave force and the second peak is attained. The wave forces reach their peaks at second 1.4. In the meantime, pressure gauge P_{2,f} (Figure 7c) attains its peak value but the pressures at P_{2,b}, P_{3,f}, P_{3,b}, P_{4,f} and P_{4,b} are recorded initially with small negative values consistently in all tests. The deflected column of water collapses, falls back on the wave with substantial amount of entrained air. The wave then overtops the bridge deck and travels away from the bridge model (Figures 8e - 8h).

One may observe from Figures 6 and 7 that the maximum wave force on the bridge model almost coincides with the occurrence of the peak net pressure at girder G1. Girder G1 is subjected to the highest wave forces compared to the others (girders G2 and G3) because it is exposed to the direct wave attack. The maximum pressure which is 2.9 times the hydrostatic pressure are obtained at the front face of girder G1. Compared to girder G1, the net pressures on girders G2 and G3 are insignificant, especially when the maximum forces are gained. It is also observed that the pressures at the back faces of girders G1, G2 and G3 pick up slightly earlier than the pressures at the front faces.

4. Numerical modeling

Numerical simulations were performed subsequently to further investigate tsunami flow around inland bridges. To ensure the appropriateness of the numerical model in simulating tsunami flow, wave flume experiments (under free flow condition without the bridge model) as performed in the experiment during calibration was reproduced numerically using a two-dimensional (2D) model as the first step. It was then followed by a detailed investigation of tsunami flow around the bridge model using a three-dimensional (3D) numerical model. The 3D model is then extended to the prototype scale in order to simulate the real flow mechanics around the target bridge prototypes.

4.1 Reviews on related numerical simulation

Several numerical studies of tsunami forces on bridges have only been conducted such as Nimmala et al. (2006), Endoh & Unjoh (2006), Ikari & Gotoh (2007), Lau et al. (2009), Murakami et al. (2009), Shigihara et al. (2009a and 2009b), Kosa et al. (2009) and Usui et al. (2010). Numerical studies on bridges subjected to tsunamis were carried out by Nimmala et al. (2006), Endoh & Unjoh (2006) and Ikari & Gotoh (2007). Nimmala's work focused on the determination of the design tsunami force on a real bridge in Oregon, U.S. under the predicted tsunami scenarios from the fault models. A two-dimensional bridge deck model (simplified as a rectangular box with top rounded edges) was considered. The fluid-structure interaction analysis of the bridge was conducted using the state-of-the-art computational mechanics software. Endoh & Unjoh (2006) and Ikari & Gotoh (2007) used the particle method where the motion of the fluid is described in a Lagrangian coordinate. The former study used the Particle Flow Code to simulate an I-girder bridge in a two-dimensional model. The target bridge was located over a dry bed in Banda Aceh, subjected to 30 m high

tsunami and a constant velocity of 68 km/h. The latter study used the Moving Particle Semi-implicit (MPS) method to simulate tsunami flow around a simplified rectangular box girder bridge over a wet bed based on the experimental study by Shoji & Mori (2006). Both studies reproduced the failure mechanism of bridges subjected to tsunami attacks.

4.2 Numerical study

The state-of-the-art Computational Fluid Dynamics (CFD) program, Flow-3D[®], was used to simulate tsunami flow around I-girder bridges. A detailed investigation of tsunami flow around the bridge model as in the experiments was carried out.

4.2.1 Numerical methodology

Flow-3D[®] is a general purpose CFD package that is used to solve transient and three-dimensional flow problems. It was developed by Flow Science, Inc., formed by Dr. C. W. Hirt in 1980, and first released in 1985 and has a comprehensive track record in CFD modeling. Though, the application in modeling tsunami on bridges is a new attempt. Flow-3D[®] is developed based on the fractional volume of fluid (VOF) free surface tracking method as discussed in Hirt & Nichols (1981). Under this method, cells are defined with a value between zero and one for empty to fully filled cells with fluid. For partially filled cells, the slope of the free surface is determined by an algorithm that uses the surrounding cells to define a surface angle and a surface location. This method allows the steep fluid slopes to be defined and it is applicable to describe the breaking wave (bore or surge) in tsunami run-up zone.

The model constructed in this research is an incompressible and viscous flow model. Flow-3D[®] employs the finite-volume method to solve the fluid equations of motion of the time dependent Reynolds Averaged Navier-Stokes (RANS). The computational domain is defined in a fixed rectangular grid or structured system. The fluid momentum equations, Navier-Stokes equations, can be expressed as follows (Flow-3D, 2007),

$$\frac{\partial u}{\partial t} + \frac{1}{V_F} \left(uA_x \frac{\partial u}{\partial x} + vA_y \frac{\partial u}{\partial y} + wA_z \frac{\partial u}{\partial z} \right) = -\frac{1}{\rho} \frac{\partial p}{\partial x} + g_x + f_x \quad (1a)$$

$$\frac{\partial v}{\partial t} + \frac{1}{V_F} \left(uA_x \frac{\partial v}{\partial x} + vA_y \frac{\partial v}{\partial y} + wA_z \frac{\partial v}{\partial z} \right) = -\frac{1}{\rho} \frac{\partial p}{\partial y} + g_y + f_y \quad (1b)$$

$$\frac{\partial w}{\partial t} + \frac{1}{V_F} \left(uA_x \frac{\partial w}{\partial x} + vA_y \frac{\partial w}{\partial y} + wA_z \frac{\partial w}{\partial z} \right) = -\frac{1}{\rho} \frac{\partial p}{\partial z} + g_z + f_z \quad (1c)$$

where u , v and w are the velocities in the x -, y - and z -directions; V_F represents the volume fraction of fluid in each cell; A_x , A_y and A_z are the fractional areas open to flow in the x -, y - and z -directions; ρ is the fluid density; p is the fluid pressure; g_x , g_y and g_z are the body accelerations in the x -, y - and z -direction and f_x , f_y and f_z are the viscous accelerations in the x -, y - and z -direction for which a turbulence model is required for closure. For cells fully filled of fluid, V_F , A_x , A_y , and A_z equal to one.

For an incompressible fluid, the following condition (i.e. continuity equation) must hold:

$$\frac{\partial}{\partial x}(uA_x) + \frac{\partial}{\partial y}(vA_y) + \frac{\partial}{\partial z}(wA_z) = 0 \quad (2)$$

Boundary conditions are categorized as symmetry, rigid-free or no-slip walls, continuative outflow, periodic and specific pressure boundaries. No flux is allowed to cross the symmetry and wall boundary; however, viscous shear stresses occur at the wall boundary only. Flow variables (velocity, pressure, etc) are constant across boundary (zero gradient). A continuative boundary condition consists of zero normal derivatives at the boundary for all flow quantities; thus, there is no acceleration or deceleration of the flow as it crosses the boundary. Free slip is defined as zero normal velocity component with zero tangential velocity derivatives ($v = 0$ and $\partial u/\partial x = \partial w/\partial z = 0$). No slip is defined as zero tangential and normal velocities ($u = v = w = 0$).

Hydraulic forces that fluid flow exerts on the solid structures are calculated by integrating the pressure acting on these structures over the open surface. Hydraulic forces which comprise the pressure and viscous forces are defined as

$$F = \int p \bar{n} dA + \int \bar{\tau} dA \quad (3)$$

where p is the pressure, dA is the solid surface area in the cell, \bar{n} is the unit vector normal to area dA and $\bar{\tau}$ is the shear stress vector.

The computational domain was discretized into an orthogonal and staggered grid of variable-sized hexahedral meshes in a Cartesian coordinates. Due to the complex bridge model, multi-block gridding with nested and linked grids (will be explained in Section 4.2.2) were applied in order to reduce the computational cost while maintaining the accuracy of the results. Also due to symmetrical orientation, only half of the wave flume was modeled. Under this discrete structural grid system, average values of the flow parameters were placed at the center of each cell (for pressure and fractional volume of fluid) and the center of cell faces normal to their associated direction (for velocity).

The basic algorithm for the computation consists of three main steps. The first step is the computation of flow velocity based on the initial conditions or previous time-step values from the explicit approximations of Navier-Stokes Equations. Next, the pressure values will be adjusted to satisfy the continuity equation. It is followed by the determination of the fluid free surface or interface and update of the new fluid configuration based on the VOF method. This computation is then advanced to the next time-step and those three steps are repeated.

On top of that, bridge and other auxiliary structures were constructed as obstacles in the numerical model. The flow obstacle was defined using a porosity technique in rectangular cell meshes called the Fractional Area/Volume Obstacle Representation (FAVOR) method as outlined in Hirt & Sicilian (1985). For cells without obstacle, the grid porosity is one and the fluid dynamic equations are to be hold. In contrast, the grid porosity is zero for cells within obstacle where no flow volume is allowed in the obstacle region. For cells that are partially filled with an obstacle, the grid porosity has a value between zero and one, based on the percent volume that is open. The surface angle and the surface location are determined based on the same principal of VOF as stated in the above section.

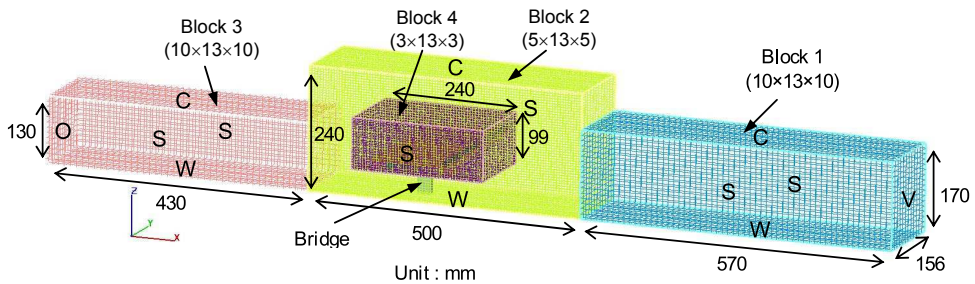
4.2.2 Computational model

Three-dimensional bridge models were constructed in the computational domain of 1.5 m long by 0.24 m high (maximum) by 0.156 m width as shown in Figure 9. The computational domain consisted of three linked blocks (Blocks 1, 2 and 3) and a nested block (Block 4) of

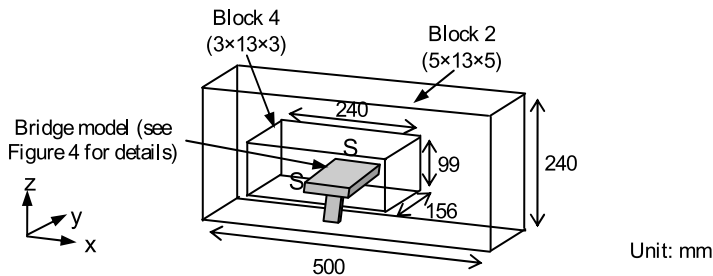
meshes as highlighted in Figure 9. The bridge model was located in Block 2 where the bridge deck was enclosed in Block 4 with higher resolution meshes as listed in Table 1. Six different boundaries of each block were defined. Sidewalls were defined as free slip/symmetry (S), the bed was no slip/wall (W); the top was continuative (C); the upstream and downstream were velocity boundary (V) and the outlet (O), respectively.

The bridge model as shown in Figure 4 was installed at the location of about 0.9 m from the right boundary. The calculation was first carried out under the free flow condition (the case without bridge model) and followed with the case with the bridge model placed on a dry bed as performed in the experiment.

Newtonian viscosity with renormalized group (RNG) $k-\epsilon$ turbulence model was adopted. The inflow properties were input at the upstream (right) boundary with time-dependent velocity and flow depth data, assuming these quantities were uniformly distributed along the width and the height of the flume at each time step. The other numerical input data were set as 1000 kg/m^3 for fluid density, 1.225 kg/m^3 for air density, 0.001 kg/m/s for fluid viscosity and -9.81 m/s^2 for gravitational acceleration. The simulated wave represented the wave propagation over a $1/115$ bed slope at near-shore. The wave hits the model at the right angle to the longitudinal axis of the bridge.



(a) Linked block



(b) Nested block

Note: Mesh size is shown in parentheses ($\Delta x \times \Delta y \times \Delta z$)

Notations for boundary condition: S - symmetry; W - wall; C - continuative; V - velocity; O - outlet

Fig. 9. Computational domain

Block	Type	Total Length (m)			Interval (mm)		
		x	y	z	Δx	Δy	Δz
1	Linked	0.57	0.156	0.17	10	13	10
2	Linked	0.5	0.156	0.24	5	13	5
3	Linked	0.43	0.156	0.13	10	13	10
4	Nested	0.24	0.156	0.099	3	13	3

Table 1. Mesh properties for bridge model

4.2.3 Model validation

Due to the complexity of the problem and the scarcity of the theoretical background in the current research focus at this stage, the only available method to ensure the appropriateness of the computational model is through the comparison of the computed results with the independent data measured from the physical modeling. Figure 10 highlights the wave profile from the numerical simulation when the generated wave strikes the model at selected time intervals. The phenomena of the wave impingement on the bridge model as those observed in the experiments (as shown in Figure 8) are well simulated in the numerical analysis.

Wave pressures were measured in the front center face of the pier at a point of 0.5 cm above the bed (P1,f) and the front and back face of girders at mid-span of the girders and 6.35 cm above the bed (P2,f and P2,b) as shown in Figure 4. For better representation, all pressure values are normalized with the nominal flow depth (maximum water level at the location of interest). The normalized pressure time histories obtained from the physical and numerical models are compared in Figure 11 while the time histories of the total horizontal force acting on the entire bridge model are shown in Figure 12. The variations of the calculated and the measured results are not significant.

It should be noted that the vertical force computed by the numerical model is not validated due to the unavailable measured data. Good agreement of the pressures and the force throughout the considered time domain has evidently justified that this numerical bridge model can reproduce the physical bridge model with high confidence. As a result, this qualitatively and quantitatively validated model is extended for the simulation of bridge prototypes as discussed in the following section.

4.2.4 Simulation of bridge prototype

This section presents simulation results of bridge prototypes subject to the scenario flow depth (H) of 8 m. Bridge prototypes are constructed by scaling up bridge models with the length scale of 100. The grid size in the numerical model is also scaled up to 100 times that in the downscaled model. To develop the generalized force and pressure distributions on the bridge deck, seven types of bridge prototypes namely CR36, CR41, CR46, CR51, CR56, CR66 and CR76 that correspond to the deck clearances (h) of 3.6 m, 4.1 m, 4.6 m, 5.1 m, 5.6 m, 6.6 m and 7.6 m are employed. The ratio of the deck clearance to the nominal flow depth (h/H) of these prototypes ranges from 0.45 to 0.95 (Table 2). The required time to complete the running time of 50 s at 0.5 s interval in the Intel® Core™ 2 Duo processor with a 3.16GHz and an 8GB RAM's computer for all cases are given in Table 2.

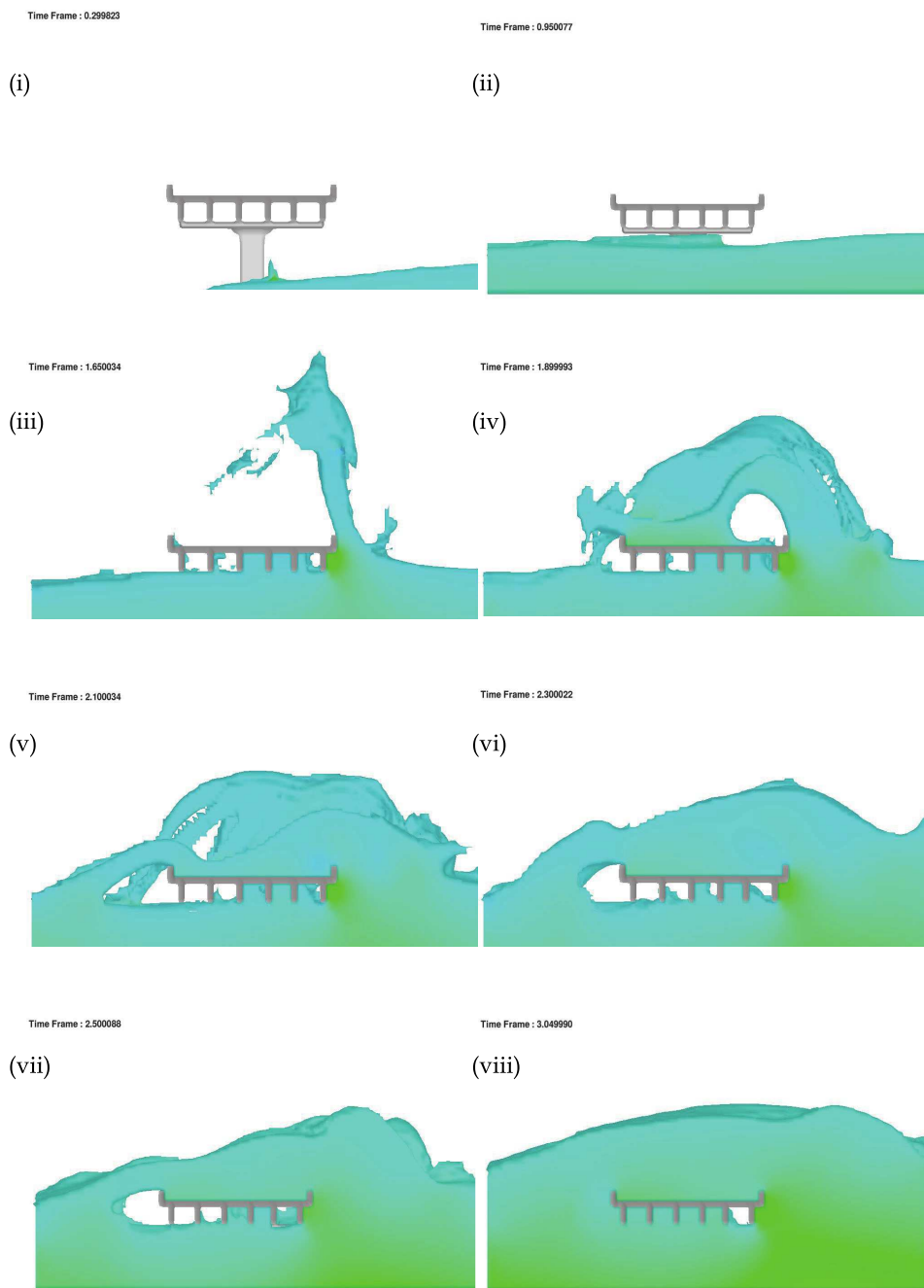
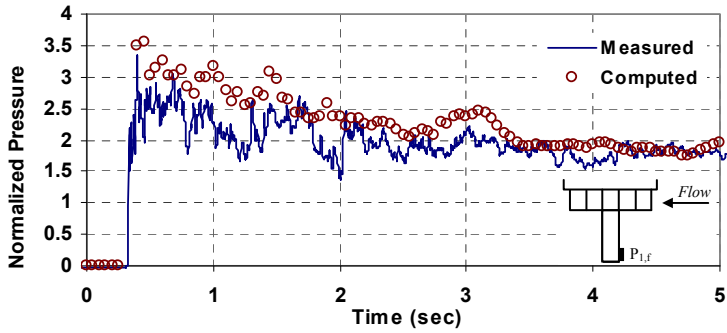
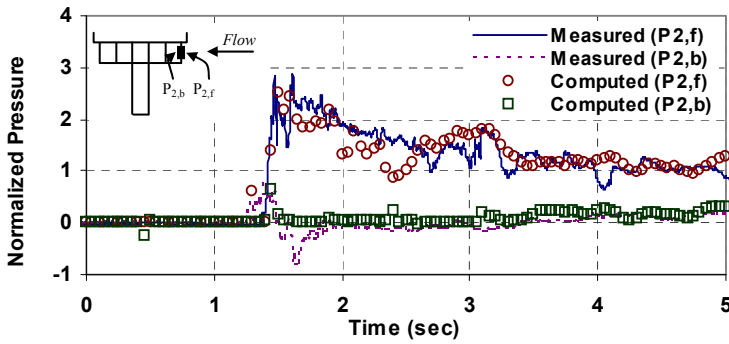


Fig. 10. Sequential events of wave impingement on a bridge model from numerical simulation



(a) P1,f



(b) P2

Fig. 11. Time histories of front face pressure on (a) pier, and (b) front girder

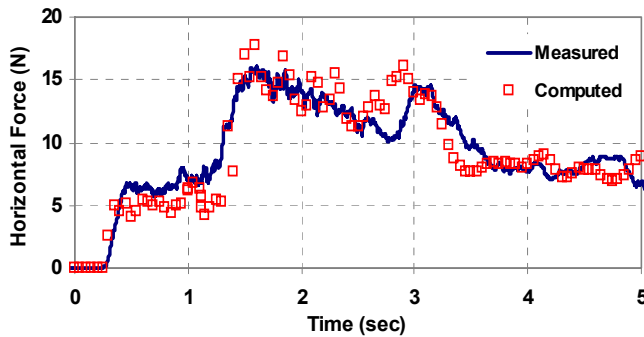


Fig. 12. Time histories of the force on bridge model

Cases	Deck Clearance, h (m)	h/H	Computational Time
CR36	3.6	0.45	8 hours 44 minutes
CR41	4.1	0.5125	9 hours 38 minutes
CR46	4.6	0.575	7 hours 32 minutes
CR51	5.1	0.6375	7 hours 50 minutes
CR56	5.6	0.70	7 hours 21 minutes
CR66	6.6	0.825	6 hours 24 minutes
CR76	7.6	0.95	4 hours 57 minutes

Table 2. h/H ratio and computational time

4.3 Computed wave pressures and forces

The pressures distribution along the height of the girders discussed in the following are normalized with the hydrostatic pressure based on the scenario flow depth of 8 m. Figure 13 presents the vertical pressure distribution at the front face of the bridge deck of seven deck clearances. As the unique configuration of the I-beam girder deck where the parapets protrude from the vertical planes of the front and back girders, the pressure distribution discontinues at the slab level ($z/H = 0.6375$ for CR36, 0.7 for CR41, 0.7625 for CR46, 0.825 for CR51, 0.8875 for CR56, 1.0125 for CR 66 and 1.1375 for CR76). As anticipated, the higher the deck, the smaller the maximum pressure is attained. The maximum normalized pressure of larger than 4 is observed for CR36 and CR41 while the normalized pressure for CR66 is below 2. When the wave initially hits the front girder or front parapet, some proportions of the hydrostatic pressure impart on the front face of the girder and parapet. Thereafter, the wave flows through the deck and it exerts almost uniform pressure over the height of the deck (except near to the free ends at the top and bottom of the deck) especially when the wave becomes nearly steady (about second 40). At the instant when the maximum wave force is attained, the pressures on the front girder and front parapet are practically dominated by the hydrodynamics and hydrostatic pressures, respectively.

Computed time histories of total horizontal and vertical forces on bridge decks subject to tsunamis with the scenario flow depth of 8 m are shown in Figure 14. The positive sign in the horizontal force represents the force in line with the flow direction while the positive and negative signs in vertical force represent the vertical uplift and the additional gravity force, respectively. The horizontal force can be generally characterized into two types, i.e. impulsive and slow-varying forces. Force measurement is firstly recorded for CR36, followed by CR41, CR46, CR51, CR56, CR66 and CR76. Impulsive forces vary substantially from case to case up to second 20 except the cases of CR66 and CR76 ($h/H \geq 0.825$) where practically no impulsive forces are recorded (Figure 14a). The peaks of the impulsive forces in the horizontal direction are obtained at second 10 (CR36), second 14.5 (CR41 and CR46) and second 16 (CR51 and CR56), which mark approximately 2 to 3 times the slowly-varying forces. As oppose to impulsive forces, all cases (except CR76) have the similar horizontal slowly-varying forces regardless their deck clearance after second 35, i.e. about 7 MN.

Vertical force time histories (Figure 14b) exhibit different trends. The vertical uplift force is firstly exerted on the deck and it followed by the additional gravity force after the wave falls on and overtops the deck. The uplift force is denoted by positive value whereas the additional gravity force is denoted by negative value based on the sign convention in the computation. CR36 and CR46 show longer period of vertical uplift force action up to

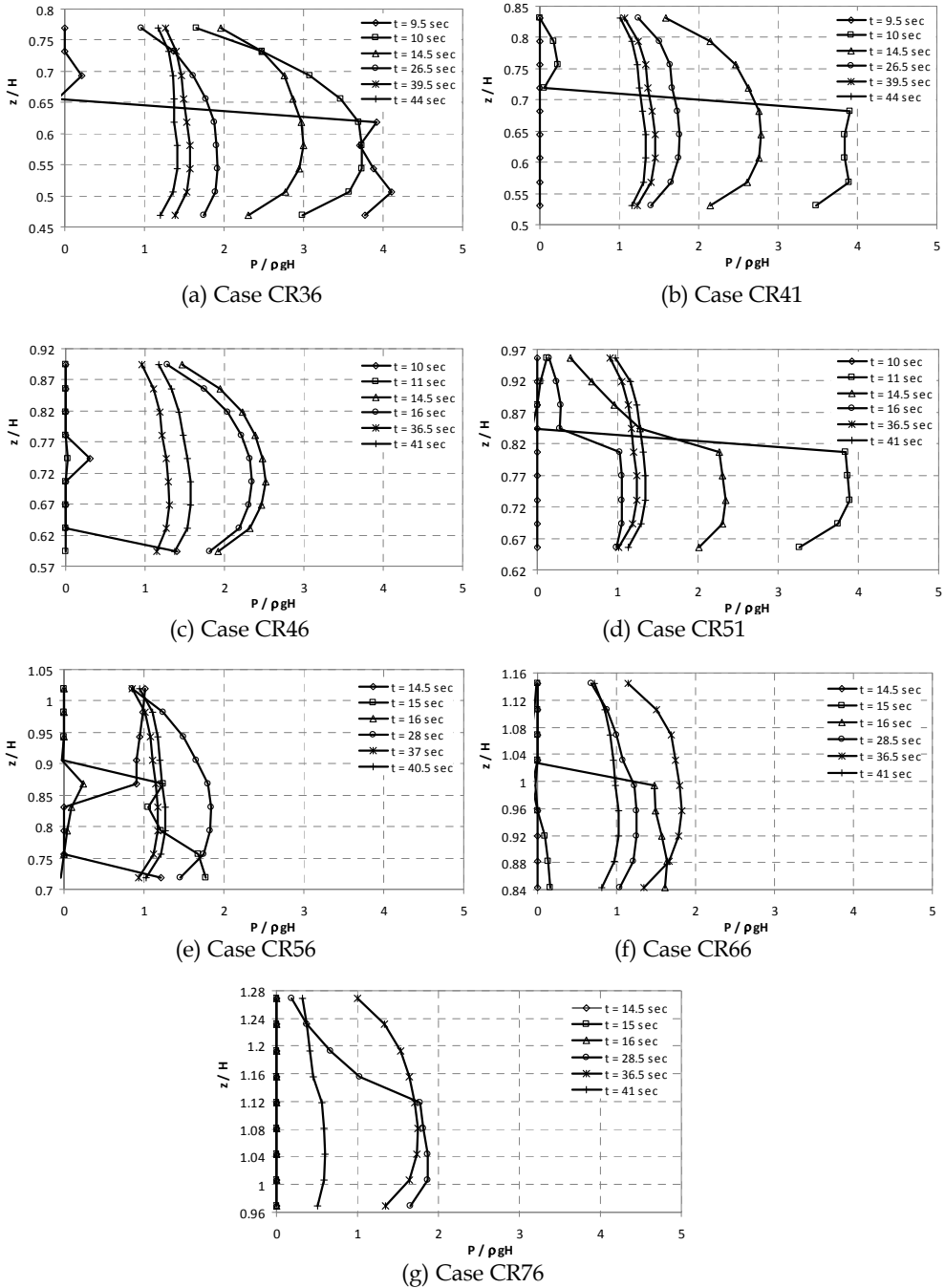
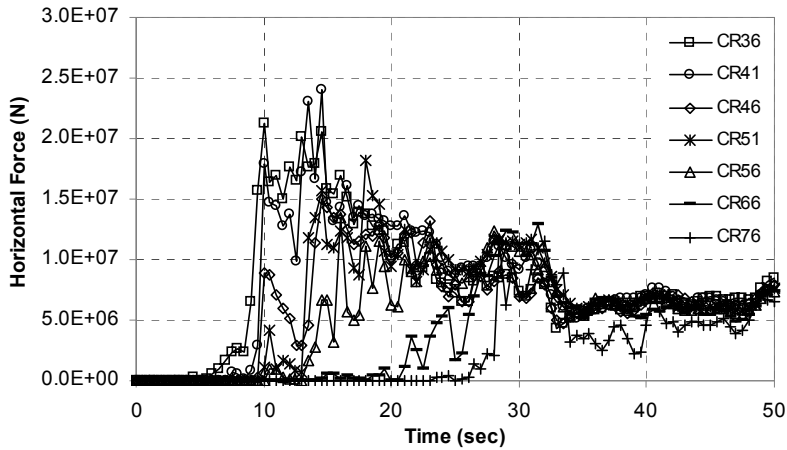
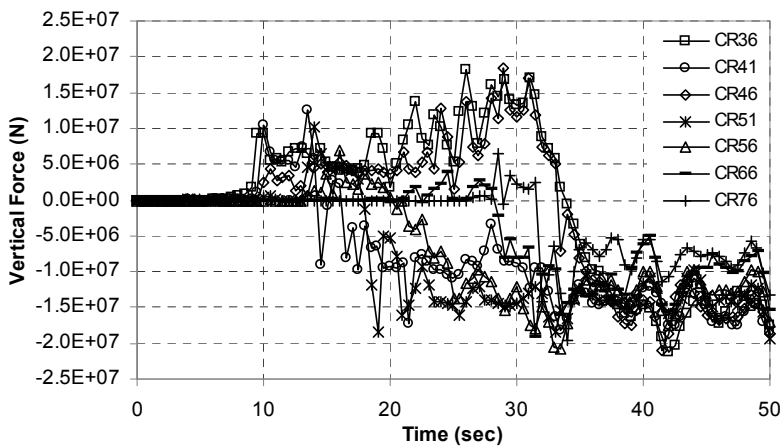


Fig. 13. Vertical pressure distributions at mid-span

second 34. This is due to the water jet (that is pushed upward) drops beyond the deck. For the case of CR41, the water jet is pushed almost upright and it drops on the deck soon after. The maximum vertical uplift forces are attained from 3.8 MN (CR66) to 18.5 MN (CR46) or 0.5 to 2.6 times the slowly-varying forces. CR66 and CR76 have relatively small vertical uplift forces. Similar to the horizontal force time history, the variation of the vertical force is not significant after second 35, where the wave with much higher flow depth flows through the bridge deck at nearly steady state. The maximum additional gravity force marks about 21 MN which is 3 times the horizontal slowly-varying force.



(a)



(b)

Fig. 14. Time histories of total force in horizontal (a) and vertical (b) components

From the results, it is observed that the front girder suffers the highest wave pressure. Therefore, it is the most critical member of the bridge deck subjected to tsunami flow. To avoid the bridge deck from washing away, it is recommended to reinforce the front girder

so that it is strong enough to withstand both the horizontal and vertical forces acting on it. The other method to reduce the tsunami forces on bridges is to reduce the exposed area to tsunami by using the perforated bridge deck as presented in Lau *et al.* (2010).

5. Tsunami force estimation

Based on the results from the numerical analysis, the formulation of tsunami wave forces on bridges is presented in this section. A method of tsunami force estimation is proposed. Tsunami forces in horizontal and vertical components are derived. Horizontal forces are categorized into peak and slowly-varying forces whereas vertical forces are categorized into uplift and additional gravity forces.

5.1 Estimation of slowly-varying forces on bridge decks

One of the important observations shown in the horizontal force time-histories (Figure 14a) are the independency of the slowly-varying forces from the deck clearance. This argument holds for h/H between 0.45 and 0.825. Pressure distributions of the slowly-varying forces on the bridge decks subject to 8 m scenario flow depth are presented in Figure 15. At the instant the slowly-varying force acts on the front face of the deck, the back face of the deck is subjected to the wave attack as well. Front and back face pressure distributions are presented in Figures 15a and 15b, respectively. It is found that the distributions can be regarded as somewhat hydrostatic. The mean values are determined from the linear least square approximation. Also plotted are the values of mean plus one standard deviation (mean + 1SD) and mean plus two standard deviations (mean + 2SD) corresponding to 68 % and 95 % confidence levels, respectively.

For the mean value the triangular shaped of the pressure distribution on the front face of the deck (Figure 15a) marks $2.48\rho gH$ on the ground and acting up to $1.64H$. The pressure distribution of the wave at the back face of the deck is shown in Figure 15b where the distribution of $0.96\rho gH$ on the ground and acting up to $1.12H$ are obtained. The wave pressure at the back face of the deck is almost similar to the hydrostatic pressure. By subtracting the back face pressure from the front face pressure, the net dimensionless pressure acting on the bridge deck are determined which can be expressed in the bilinear relationships as follows,

For mean,

$$P = \rho gH (2.3246 - z/H) / 1.5302, \quad 0.4 \leq z/H \leq 1.12 \quad (4a)$$

$$P = \rho gH (1.642 - z/H) / 0.6626, \quad 1.12 \leq z/H \leq 1.3 \quad (4b)$$

Similarly,

For mean + 1SD,

$$P = \rho gH (2.4168 - z/H) / 1.5302, \quad 0.4 \leq z/H \leq 1.16 \quad (4c)$$

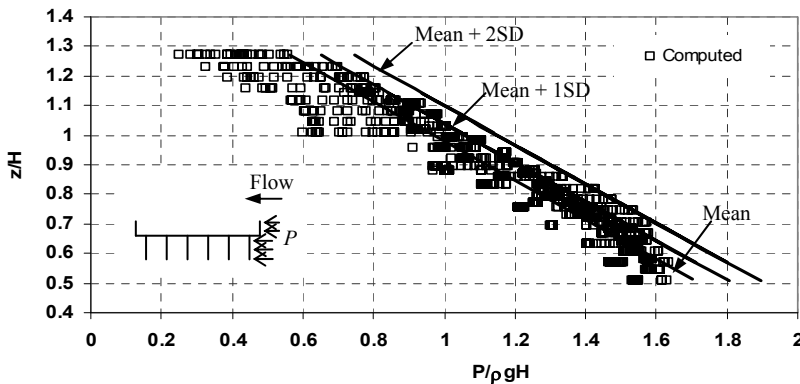
$$P = \rho gH (1.7024 - z/H) / 0.6626, \quad 1.16 \leq z/H \leq 1.3 \quad (4d)$$

For mean + 2SD,

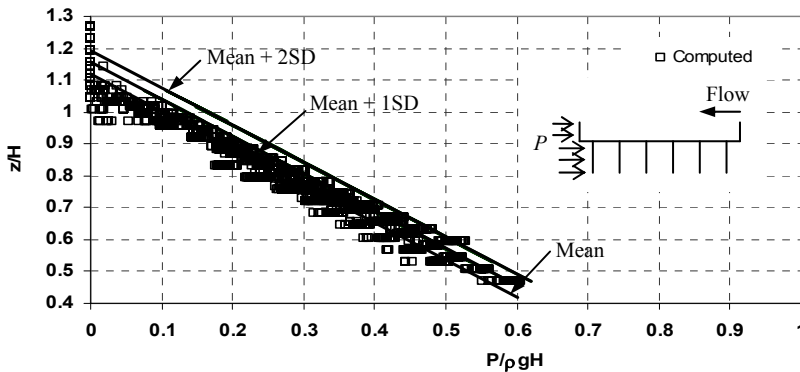
$$P = \rho gH (2.5093 - z/H) / 1.5302, \quad 0.4 \leq z/H \leq 1.19 \quad (4e)$$

$$P = \rho g H (1.7628 - z/H) / 0.6626, \quad 1.19 \leq z/H \leq 1.3 \tag{4f}$$

where z is the height of the point of interest that is measured from the ground level. Eq. (4a) to Eq. (4f) are used to calculate the forces acting on the bridge decks with various clearances within the limits of the deck heights. Except for the cases which the decks are placed at extreme low and high position (CR36 and CR76), the results indicate that the mean + 2SD pressure distribution can adequately predict slowly-varying forces.



(a) Front face pressure distribution



(b) Back face pressure distribution

Fig. 15. Distribution of slowly-varying pressure on front (a) and back (b) faces of bridge deck

5.2 Proposed formulae for predicting tsunami forces on bridge decks

To make the prediction of the horizontal impulsive, vertical uplift and additional gravity forces possible, the method for estimating coastal wave forces on bridge decks suggested by Douglass et al. (2006) is proposed. This approach has been adopted in the Federal Highway Administrative Hydraulic Engineering Circular No. 25 (HEC-25, 2008). The fundamental idea of this approach is to determine the reference forces in the horizontal and vertical components which are ‘apparent hydrostatic forces’ and the maximum impact forces

correspond to those components are then computed as some multiple of these reference forces.

The reference forces stipulated in HEC-25 (2008) which based on the level of submergence are not applicable for broken waves (tsunami bores or surges) because the crest of the wave is not easily predicted using the current knowledge. Therefore, the reference forces based on the pressure distribution of slowly-varying forces derived in Section 5.1 are proposed for tsunami cases. The selection of the slowly-varying force as the reference force is the appropriate one due to the aforementioned characteristics of: (1) independency from the deck clearance; (2) occur at near steady state flow region; and (3) insignificance of forces on the intermediate girders.

This reference forces are associated to the height of the deck and the scenario flow depths which are known values. The reference force, F_{ref} , is expressed as

$$F_{ref} = PA \quad (5)$$

where P = the pressure acting on the deck that can be estimated from Eq. (4), and A = the vertical projected area of the deck.

The maximum forces acting on bridge decks, i.e. horizontal slowly-varying, horizontal impulsive, vertical uplift and additional gravity forces are estimated from the following expressions:

$$\text{Maximum horizontal slowly-varying force, } (F_{sv})_{max} = c_{sv}F_{ref} \quad (6a)$$

$$\text{Maximum horizontal impulsive force, } (F_{imp})_{max} = (c_{sv} + c_i)F_{ref} \quad (6b)$$

$$\text{Maximum vertical uplift force, } (F_{uplift})_{max} = (c_{sv} + c_u)F_{ref} \quad (6c)$$

$$\text{Maximum additional gravity force, } (F_{ag})_{max} = (c_{sv} + c_a)F_{ref} \quad (6d)$$

where c_{sv} = an empirical coefficient for the horizontal slowly-varying force,
 c_i = an empirical coefficient for the horizontal impulsive force,
 c_u = an empirical coefficient for the vertical uplift force, and
 c_a = an empirical coefficient for the additional gravity force.

The empirical coefficients in Eq. (6) are determined based on the numerical simulation results in the current stage of the study. Under the circumstances where the reference force subjected to high uncertainties, the coefficient of c_{sv} can be increased to a value that equivalents to the desired factor of safety. The cases considered here are limited to seven different deck clearances subject to the scenario flow depth of 8 m. For a better representation, these empirical coefficients should be refined by adequate data from the experimental and analytical simulations in the future.

The accuracy of the proposed method is evaluated and compared with the computed results from the simulation. By using the pressure distribution based on the mean + 1SD for not a conservative estimation and the empirical coefficients of $c_{sv} = 1$, $c_i = 1.5$, $c_u = 1$ and $c_a = 2$, the relations of forces predicted from the proposed formulae (Eq. 6) and the computed results from the numerical model are shown in Figure 16. The computed forces from the proposed empirical formula give close estimation with those from the numerical simulation, except for the decks with large clearances which are overestimated.

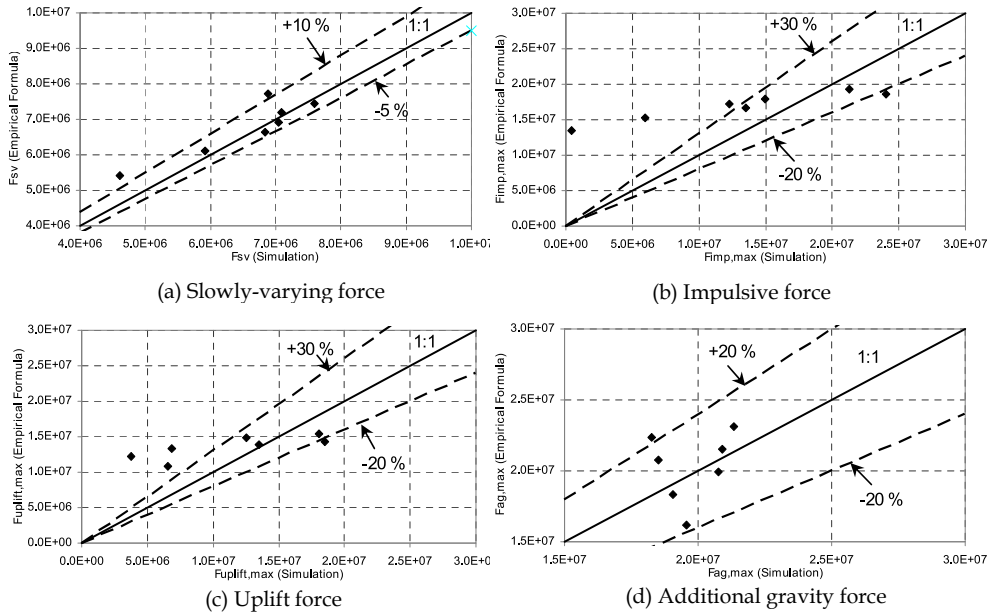


Fig. 16. Comparisons of the forces calculated from the empirical formula and numerical simulation

6. Conclusion

Both physical and numerical simulations have been carried out to investigate the behavior of bridge deck subjected to tsunamis and to formulate tsunami forces on bridge decks. Laboratory experiments give realistic insight into wave flow through the bridge model, however, small scale effect, time consuming and cost implication are the shortcomings. Numerical modeling is another powerful tool to investigate the flow mechanics around bridge decks. The well validated numerical model was employed to simulate tsunami flow around bridge prototypes to overcome the shortcomings of the physical simulation. The results reveal important findings which provide beneficial information on tsunami forces on bridges to engineers and scientists. Tsunami forces on bridge deck are categorized into four types, i.e. impulsive, slowly-varying, uplift and additional gravity forces. A method to predict the maximum values of these forces are proposed.

7. Acknowledgments

The authors would like to express sincere gratitude to the JICA AUN/SEED-Net Project for funding this research. Special thanks are also extended to Asst. Prof. Dr. Anat Ruangrassamee, Mr. Nuttawut Thanasisathit and Mr. Surakai Bachuen. The facility and assistance provided at Asian Institute of Technology and Tokyo Institute of Technology are highly appreciated.

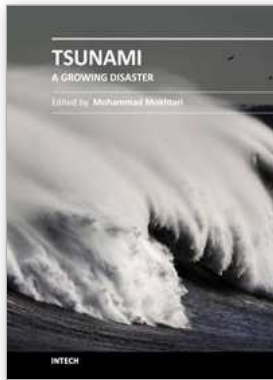
8. References

- Araki, S., Nakajima, Y., Deguchi, I. & Itoh, S. (2008). Experimental Study on Tsunami Fluid Force Acting on Bridge Beam near River Mouth, *Annual Journal of Coastal Engineering*, JSCE, Vol.55, pp. 866-870 (in Japanese)
- Araki, S., Sakashita, Y. & Deguchi, I. (2010). Characteristics of Horizontal and Vertical Tsunami Force Acting on Bridge Beam, *Annual Journal of Coastal Engineering*, JSCE, Vol. B2-66, pp. 796-800 (in Japanese)
- Ballantyne, D. (2006). Sri Lanka Lifelines after the December 2004 Great Sumatra Earthquake and Tsunami, *Earthquake Spectra*, Vol.22(S3), pp. S545-559, ISSN 8755-2930
- Camfield, F.E. (1994). Tsunami Effects on Coastal Structures, In *Coastal Hazards: Perception, Susceptibility and Mitigation*, *Journal of Coastal Research*, Special Issue No. 12, pp. 177-187, ISSN 0749-0208
- Douglass, S.L., Chen, Q.J., Olsen, J.M., Edge, B.L. & Brown, D. (2006). *Wave Forces on Bridge Decks*, U.S. Department of Transportation, Federal Highway Administration
- EEFIT. (2006). *The Indian Ocean Tsunami of 26 December 2004 : Mission Findings in Sri Lanka and Thailand*, Earthquake Engineering Field Investigation Team (EEFIT), ISBN 0-901297-41-0, United Kingdom, Austria
- Flow-3D. (2007). *Flow-3D User Manual: Excellence in Flow Modeling Software*, v9.2, Flow Science, Inc., Santa Fe, N.M
- HEC-25. (2008). *Highways in the Coastal Environment*, hydraulic Engineering Circular No. 25, Second Edition, Ed. Douglass, S.L. & Krolak, J., Federal Highway Administration, Publication No. FHWA-NHI-07-096
- Hirt, C.W. & Nicholas, B.D. (1981). Volume of Fluid (VOF) Method for the Dynamics of Free Boundaries, *Journal of Computational Physics*, Vol.39, pp. 201-225
- Hirt, C.W. & Sicilian, J.M. (1985). A Porosity Technique for the Definition of Obstacles in Rectangular Cell Meshes, *Proceedings of the 4th International Conference on Ship Hydrodynamics*, National Academic of Science, Washington, D.C., pp. 1-19
- Iemura, H., Pradono, M.H. & Takahashi, Y. (2005). Report on the Tsunami Damage of Bridges in Banda Aceh and Some Countermeasures, *Proceedings of the 28th JSCE Earthquake Engineering Symposium*, Tokyo, August, 2005, ISSN 1880-4624
- Iemura, H., Pradono, M.H., Yasuda, T. & Tada, T. (2007). Experiments of Tsunami Force Acting on Bridge Models, *Journal of Earthquake Engineering*, JSCE, Vol.29, pp. 531-536
- IIIT. (January 2011). *Quick Report on the Study of the 2004 Sumatra Earthquake and Tsunami Effects*, Department of Civil Engineering, Indian Institute of Technology Kanpur, 06.01.2011, Available from

- http://www.eeri.org/lfe/clearinghouse/sumatra_tsunami/reports/Quick_Report_Complete_India.pdf
- Ikari, H. & Gotoh, H. (2007). Numerical Simulation of Washed Process of Girder Bridge by Tsunami Run-up, *Annual Journal of Coastal Engineering*, JSCE, Vol.54, pp. 211-215 (in Japanese)
- Jain, S.K.; Murty, C.V.R., Rai, D.C., Malik, J.N., Sheth, A. & Jaiswal, A. (2005). Effects of M9 Sumatra Earthquake and Tsunami of 26 December 2004, *Current Science*, Vol.88, No.3, pp. 357-359, ISSN 0011-3891
- Kataoka, S., Kusakabe, T. & Nagaya, K. (2006). Wave Forces Acting on Bridge Girders Struck by Tsunami, *Proceedings of the 12th Japan Earthquake Engineering Symposium*, pp. 154-157, Tokyo, Japan, November 3-5, 2006 (in Japanese)
- Kusakabe, T., Matsuo, O. & Kataoka, S. (2005). Introduction of a Methodology to Mitigate Tsunami Disaster by the Pre-Evaluation of Tsunami Damage Considering Damage Investigation of 2004 Tsunami Disaster in the Indian Ocean, *Proceedings of the 21st US-Japan Bridge Engineering Workshop*, Tsukuba, Japan, October 3-5, 2005
- Lau, T.L., Lukkunaprasit, P., Ruangrassamee, A. & Ohmachi, T. (2008). Physical Modeling: An Estimation of Wave Forces on an Inland Bridge Subject to Tsunami Bores, *Proceedings of the 5th International Conference on Urban Earthquake Engineering*, pp. 441-446, Tokyo, Japan, March 4-5, 2008
- Lau, T.L., Lukkunaprasit, P., Ruangrassamee, A. & Ohmachi, T. (2010). Performance of Bridge with Solid and Perforated Parapets in Resisting Tsunami Attacks, *Journal of Earthquake and Tsunami*, Vol.4, No. 2, pp. 95-104, ISSN 1793-4311
- Lau, T.L., Ohmachi, T. & Inoue, S. (2009). Numerical Simulation of Tsunami Flow around I-Girder Bridge Decks, *Proceedings of the 6th International Conference on Urban Earthquake Engineering*, pp. 823-828, Tokyo, Japan, March 3-4, 2009
- Lukkunaprasit, P. & Lau, T.L. (2011). Influence of Bridge Deck on Tsunami Loading on Inland Bridge Piers, *The IES Journal Part A: Civil & Structural Engineering*, Vol.4, No.2, pp. 115-121, ISSN 1937-3260
- Maheshwari, B.K., Sharma, M.L. & Narayan, J.P. (2006). Geotechnical and Structural Damage in Tamil Nadu, India, from the December 2004 Indian Ocean Tsunami, *Earthquake Spectra*, Vol.22(S3), pp. S475-493, ISSN 8755-2930
- Moriyama, T., Shoji, G., Fujima, T., Shigihara, K. & Kasahara, K. (2008). Experimental Study Associated with Tsunami Wave Load Acting onto a Bridge Deck, *Book of Abstract for the 6th Annual Conference of the Japan Association for Earthquake Engineering*, JAEE, pp. 146-147, Sendai, Japan, November 3-5, 2008 (in Japanese)
- Nakao, H., Izuno, K. & Koyabashi, H. (2009). Hydrodynamic Force on Bridge Deck Models Subjected to Tsunami, *Journal of Earthquake Engineering*, JSCE, Vol.30, pp. 914-920 (in Japanese)
- Narayan, J.P.; Sharma, M.L. & Maheshwari, B.K. (2005). Effects of Medu and Coastal Topography on the Damage Pattern during the Recent Indian Ocean Tsunami along the Coast of Tamilnadu, *Science of Tsunami Hazards*, Vol.23, No.2, pp. 9-18, ISSN 8755-6839

- Nii, S., Kosa, K., Shoji, G. & Kimura, K. (2009). Experimental Examination Concerning Tidal Wave Action Power to Bridge, *Journal of Structural Engineering*, JSCE, Vol.55A, pp. 471-482 (in Japanese)
- Nii, S., Kosa, K., Shoji, G. & Kimura, K. (2010). Experimental Examination Concerning the Tsunami Wave Force to Bridge by Difference of the Wave Shape, *Journal of Structural Engineering*, JSCE, Vol.56A, pp. 474-485 (in Japanese)
- Nimmala, S.H., Yim, S.C., Cheung, K.F. & Wei, Y. (2006). Tsunami Design Criteria for Coastal Infrastructure: A Case Study for Spencer Creek Bridge, Oregon, Oregon Department of Transportation
- Saatcioglu, M.; Ghobarah, A. & Nistor, I. (2005). Effects of the December 26, 2004 Sumatra Earthquake and Tsunami on Physical Infrastructure, *ISET Journal of Earthquake Technology*, Vol.42, No.4, pp. 79-94, ISSN 0972-0405
- Scawthorn, C., Ono, T., Iemura, H., Ridha, M. & Purwanto, B. (2006). Performance of Lifelines in Banda Aceh, Indonesia, during the December 2004 Great Sumatra Earthquake and Tsunami, *Earthquake Spectra*, Vol.22(S3), pp. S511-544, ISSN 8755-2930
- Sheth, A., Sanyal, S., Jaiswal, A. & Gandhi, P. (2006). Effects of the December 2004 Indian Ocean Tsunami on the Indian Mainland, *Earthquake Spectra*, Vol.22(S3), pp. S435-473, ISSN 8755-2930
- Shoji, G. & Mori, Y. (2006). Hydraulic Model Experiment to Simulate the Damage of a Bridge Deck Subjected to Tsunamis, *Annual Journal of Coastal Engineering*, JSCE, Vol.53, pp. 801-805 (in Japanese)
- Shoji, G., Hiraki, Y., Fujima, K., & Shigihara, Y. (2010). Experimental Study on Fluid Force Acting on a bridge Deck Subjected to Plunging Breaker Bores and Surging Breaker Bores, *Annual Journal of Coastal Engineering*, JSCE, Vol. B2-66, pp. 801-805 (in Japanese)
- Shoji, G., Moriyama, T., Fujima, K., Shigihara, Y. & Kasahara, K. (2009a). Experimental Study Associated with a breaking Tsunami Wave Load Acting onto a Single Span bridge Deck, *Journal of Structural Engineering*, JSCE, Vol.55A, pp. 460-470 (in Japanese)
- Shoji, G., Moriyama, T., Hiraki, Y., Fujima, K., Shigihara, Y. & Kasahara, K. (2009b). Evaluation of a Tsunami Wave load Acting on a Bridge Deck Subjected to Plunging Breaker Bores and Surging Breaker Bores, *Annual Journal of Coastal Engineering*, JSCE, Vol. B2-65, pp. 826-830 (in Japanese)
- Tobita, T.; Iai, S., Chairullah, B. & Asper, W. (2006). Reconnaissance Report of the 2004 Great Sumatra-Andaman, Indonesia, Earthquake - Damage to Geotechnical Works in Banda Aceh and Meulaboh -, *Journal of Natural Disaster Science*, Vol.28, No.1, pp. 35-41, ISSN 0388-4090
- Unjoh, S. (2005). *Damage to Transportation Facilities, The Damage Induced by Sumatra Earthquake and Associated Tsunami of December 26, 2004, A Report of the Reconnaissance Team of Japan Society of Civil Engineers*, pp. 66-76
- Yeh, H. (2007). Design Tsunami Forces for Onshore Structures, *Journal of Disaster Research*, Vol.2, No.6, pp. 531-536, ISSN 1881-2473

Yim, S.C. (2005). Modeling and Simulation of Tsunami and Storm Surge Hydrodynamics Loads on Coastal Bridge Structures, *Proceedings of the 21st US-Japan Bridge Engineering Workshop*, Tsukuba, Japan, October 3-5, 2005



Tsunami - A Growing Disaster

Edited by Prof. Mohammad Mokhtari

ISBN 978-953-307-431-3

Hard cover, 232 pages

Publisher InTech

Published online 16, December, 2011

Published in print edition December, 2011

The objective of this multi-disciplinary book is to provide a collection of expert writing on different aspects of pre- and post- tsunami developments and management techniques. It is intended to be distributed within the scientific community and among the decision makers for tsunami risk reduction. The presented chapters have been thoroughly reviewed and accepted for publication. It presents advanced methods for tsunami measurement using Ocean-bottom pressure sensor, kinematic GPS buoy, satellite altimetry, Paleotsunami, Ionospheric sounding, early warning system, and scenario based numerical modeling. It continues to present case studies from the Northern Caribbean, Makran region and Tamil Nadu coast in India. Furthermore, classifying tsunamis into local, regional and global, their possible impact on the region and its immediate vicinity is highlighted. It also includes the effects of tsunami hazard on the coastal environment and infrastructure (structures, lifelines, water resources, bridges, dykes, etc.); and finally the need for emergency medical response preparedness and the prevention of psychological consequences of the affected survivors has been discussed.

How to reference

In order to correctly reference this scholarly work, feel free to copy and paste the following:

Tze Liang Lau, Tatsuo Ohmachi, Shusaku Inoue and Panitan Lukkunaprasit (2011). Experimental and Numerical Modeling of Tsunami Force on Bridge Decks, *Tsunami - A Growing Disaster*, Prof. Mohammad Mokhtari (Ed.), ISBN: 978-953-307-431-3, InTech, Available from: <http://www.intechopen.com/books/tsunami-a-growing-disaster/experimental-and-numerical-modeling-of-tsunami-force-on-bridge-decks>

INTECH
open science | open minds

InTech Europe

University Campus STeP Ri
Slavka Krautzeka 83/A
51000 Rijeka, Croatia
Phone: +385 (51) 770 447
Fax: +385 (51) 686 166
www.intechopen.com

InTech China

Unit 405, Office Block, Hotel Equatorial Shanghai
No.65, Yan An Road (West), Shanghai, 200040, China
中国上海市延安西路65号上海国际贵都大饭店办公楼405单元
Phone: +86-21-62489820
Fax: +86-21-62489821

© 2011 The Author(s). Licensee IntechOpen. This is an open access article distributed under the terms of the [Creative Commons Attribution 3.0 License](#), which permits unrestricted use, distribution, and reproduction in any medium, provided the original work is properly cited.